J Eng Math (2010) 67:55–69
DOI 10.1007/s10665-009-9334-7

Computation formulas by FFT of the nonlinear orbital velocity in three-dimensional surface wave fields

John Grue

Received: 22 January 2009 / Accepted: 14 September 2009 / Published online: 6 October 2009

Abstract Accurate representations of the surface potential and the orbital velocity of nonlinear water waves are obtained, given the spatial wave-elevation field and its time derivative along two-dimensional sections of the ocean surface. The effect of a horizontal current is accounted for. The method is three-dimensional. The kernel of an integral equation and its right-hand side, both nonlinear functions of the elevation, are obtained in series expansions, and expressed explicitly by Fourier transform (FFT). Calculations for a periodic sine-wave and non-periodic model directional irregular wave field over swaths (wave slope in the range ± 0.3 in both cases) illustrate the formulas. The Gibbs phenomenon along the boundaries affects the very high-order contributions in the non-periodic case.

Keywords Fast Fourier transform · Orbital velocity · Surface wave fields in three dimensions · Waves on current

1 Introduction

Ocean surface waves are commonly recorded in the form of time series in single, fixed points. An example is the record obtained from a down-looking laser-based wave sensor, on the Draupner E platform in the central North Sea. This contains the famous Draupner New Year Wave, with crest a height of 18.5 m and a trough-to-trough period of 12 s, recorded on January 1, 1995 [1–3]. In a more recent method one obtains, instead, the wave elevation as a function of the spatial coordinate, at a fixed time. This strategy was pursued in airborne measurements of storm waves in the Gulf of Tehuantepec experiment (GOTEX) [4]. Elevation records over swaths 5 km long and 200 m wide were obtained as a function of the spatial coordinate, assuming that the speed of the airplane is much faster than the typical wave phase speed. Measurements obtained in the front and aft of the airplane are important features of the experiment, enabling an evaluation of the time derivative of the surface elevation. Thus, the surface elevation,

Dedication Professor Peregrine accepted an invitation as an international, internal referee of: "General analysis of Realistic Ocean Waves", a larger theoretical and experimental program at the University of Oslo. During the program period 1998–2002 he visited our group and viewed our laboratory measurements. Thanks to his considerable expertise, we got invaluable feedback on our plans and efforts. He communicated several of our papers on wave theory submitted for publication in the Journal of Fluid Mechanics. Over the years, I experienced a growing, mutual friendship with Howell.

J. Grue (✉)
Mechanics Division, Department of Mathematics, University of Oslo, Oslo, Norway
e-mail: johng@math.uio.no

η, and its time derivative, η_t, were obtained as functions of the horizontal coordinates, x_1, x_2, where x_1 denotes the coordinate along the flight direction, and x_2 the lateral coordinate.

Accurate calculation of the fluid velocities induced by the nonlinear wave field has been requested in GOTEX [5], since the wave kinematics could not be measured. The orbital velocity calculation may be regarded as a post processing of the elevation data base and is useful to improve the analysis of the measurements, interpret observed breaking events, evaluate velocities in the entire wave field (including along the vertical), derive statistics of the wave induced velocities, and compare with velocity measurements when available. With this motivation we derive calculation formulas obtaining the orbital velocity in realistic ocean wave fields such as GOTEX. The input to the calculations is the spatial wave elevation, η, and its time derivative, η_t, where both quantities are presented in the form of functions of the horizontal coordinates, x_1, x_2, over certain regions of the ocean, at fixed time. The effect of a horizontal current is accounted for. The method is three-dimensional.

The formulation is based on potential theory. Conservation of mass leads to a formulation where the motion is obtained by solving the Laplace equation with the position of the free surface given. The solution is obtained in the form of an integral equation with the velocity potential at the free surface as unknown; see Sect. 2. The analysis concerns the solution procedure of the integral equation. This has a kernel that is nonlinear in the surface elevation, η. The right-hand side of the equation is also a nonlinear function of η. These nonlinear functions, obtained in series expansions of η, are used in the inversion procedure of the integral equation, where the terms are expressed in explicit form by Fourier transform. More precisely, the terms are expressed by a sum of moments of η times the inverse Fourier transform of the wavenumber times: the Fourier transform of products between η^m and a scaled normal velocity, or free-surface potential, or the horizontal gradient of η times the free-surface potential. The final form of the integral expressions involves only the Fourier transform (FFT) and is easy to implement for numerical calculations.

The analysis in Sect. 3 is carried out for finite and infinite water depth, with solution procedure discussed in Sect. 4. The formulas are illustrated in three-dimensional calculations of a sine-wave and a model directional irregular wave field. The latter has a peak period of 10 s, a wave slope in the range ± 0.3 and extends over a swath 2,000 m by 200 m (Sect. 5). Concluding remarks are given in Sect. 6.

2 Mathematical formulation

2.1 Kinematic boundary condition at the free surface

The kinematic boundary condition at the free surface defines the normal velocity of the fluid motion at the free surface ($\partial\phi/\partial n$ – assuming potential theory). If the potential is known along the free surface, the tangential velocity can be obtained [6]. We study the motion of a wave field in three dimensions propagating in water of finite depth h. The wave field may interact with a horizontal current. Let $\mathbf{x} = (x_1, x_2)$ denote horizontal coordinates, y the vertical coordinate and t time. Let $\eta(\mathbf{x}, t)$ denote the free-surface elevation. We assume that the velocity field at any point of the fluid is decomposed by

$$\mathbf{v} = \mathbf{U} + \text{grad}\,\phi. \tag{1}$$

Here, $\mathbf{U} = (U_1, U_2)$ denotes a horizontal current. In the subsequent analysis $\mathbf{U}$ is assumed to be constant. The second term describes the wave-induced velocity field. This is assumed to be obtained by a potential-theory formulation, where $\phi(\mathbf{x}, y, t)$ denotes the velocity potential.

The kinematic boundary condition at the free surface gives

$$\frac{\partial \eta}{\partial t} + (\mathbf{U} + \nabla\phi) \cdot \nabla\eta = \frac{\partial \phi}{\partial y}, \tag{2}$$

where we have introduced the horizontal gradient by $\nabla = (\partial/\partial x_1, \partial/\partial x_2)$. Working with the velocity normal to the free surface we note that

$$\frac{\partial \phi}{\partial n} = \left(\frac{\partial \phi}{\partial y} - \nabla\phi \cdot \nabla\eta\right)\left(1 + |\nabla\eta|^2\right)^{-\frac{1}{2}}. \tag{3}$$

Combining (2) and (3) we obtain

$$\frac{\partial \phi}{\partial n}\left(1+|\nabla\eta|^2\right)^{\frac{1}{2}} = \frac{\partial \eta}{\partial t} + \mathbf{U}\cdot\nabla\eta = \frac{\partial \zeta}{\partial t}. \tag{4}$$

This defines the quantity $\zeta_t = \eta_t + \mathbf{U}\cdot\nabla\eta$ which is used in the subsequent analysis.

2.2 Integral equation to determine the wave potential: $h = \infty$

A relation to determine the wave potential at the free surface is derived from the mass-conservation principle. For simplicity we assume in this subsection that the water depth is infinite ($h = \infty$). The effect of a finite water depth is discussed in Sect. 3.3 below. We denote the value of the wave-induced velocity potential on the free surface by $\widetilde{\phi}(\mathbf{x}, t) = \phi(\mathbf{x}, y = \eta(\mathbf{x}, t), t)$, where $\eta(\mathbf{x}, t)$ denotes the surface elevation. By use of Green's theorem with an evaluation point $(\mathbf{x}, \eta)$ on the free surface, we obtain

$$\widetilde{\phi} + \frac{1}{2\pi}\int\limits_S \widetilde{\phi}'\frac{\partial}{\partial n'}\frac{1}{r}\mathrm{d}S' = \frac{1}{2\pi}\int\limits_S \frac{1}{r}\frac{\partial \phi'}{\partial n'}\mathrm{d}S'. \tag{5}$$

Here, $1/r$ denotes the three-dimensional source function where $r = |(\mathbf{x}, y) - (\mathbf{x}', y')|$ denotes the distance between the evaluation point $(\mathbf{x}, y)$ and integration point $(\mathbf{x}', y')$. A prime denotes the integration variable. The evaluation surface S corresponds to the instantaneous position of the free surface, and the unit normal is pointing out of the fluid. The surface element is $\mathrm{d}S = (1+|\nabla\eta|^2)^{\frac{1}{2}}\mathrm{d}\mathbf{x}$, where $\mathrm{d}\mathbf{x} = \mathrm{d}x_1\mathrm{d}x_2$.

Using the kinematic boundary condition (4) at the free surface, $\phi_n(1+|\nabla\eta|^2)^{\frac{1}{2}} = \zeta_t$, we obtain

$$\widetilde{\phi} + \frac{1}{2\pi}\int\limits_{\mathbf{x}'} \widetilde{\phi}'\left(1+|\nabla'\eta'|^2\right)^{\frac{1}{2}}\frac{\partial}{\partial n'}\frac{1}{r}\mathrm{d}\mathbf{x}' = \frac{1}{2\pi}\int\limits_{\mathbf{x}'}\frac{\zeta_t'}{r}\mathrm{d}\mathbf{x}', \tag{6}$$

where $\int_{\mathbf{x}'}$ denotes integration over the horizontal plane. Clamond and Grue [7, Sect. 6] and Grue [8] applied the Fourier transform to invert (6), obtaining

$$\mathcal{F}(\widetilde{\phi}) = \frac{\mathcal{F}(\zeta_t)}{k} + \mathcal{F}\left(\eta\mathcal{F}^{-1}[k\mathcal{F}(\widetilde{\phi})]\right) + \frac{\mathbf{i}\mathbf{k}}{k}\cdot\mathcal{F}(\eta\nabla\widetilde{\phi}) + \mathcal{F}(\mathcal{R}_1), \tag{7}$$

where $\mathcal{F}$ denotes the Fourier transform over the horizontal plane, $\mathcal{F}^{-1}$ is the inverse transform, $\mathbf{k} = (k_1, k_2)$ is the wavenumber in spectral space and $k = |\mathbf{k}|$. The terms contained in the remainder $\mathcal{R}_1$ were expressed by ordinary integration. Fructus et al. [9] implemented, tested and documented the method in full, and used it to study fully nonlinear evolution of various nonlinear water-wave fields, deriving the following version of the remainder $\mathcal{R}_1$ in (7) (with $\mathbf{U} = 0$)

$$\mathcal{R}_1 = \tfrac{1}{2}\eta^2\mathcal{F}^{-1}[k\mathcal{F}(\zeta_t)] - \eta\mathcal{F}^{-1}[k\mathcal{F}(\zeta_t\eta)] + \tfrac{1}{2}\mathcal{F}^{-1}[k\mathcal{F}(\zeta_t\eta^2)] + \mathcal{R}_2, \tag{8}$$

where

$$2\pi\mathcal{R}_2 = \int\limits_{\mathbf{x}'}\widetilde{\phi}'\left[(1+D^2)^{-\frac{3}{2}} - 1\right]\nabla'\cdot\left[(\eta'-\eta)\nabla'\frac{1}{R}\right]\mathrm{d}\mathbf{x}' + \int\limits_{\mathbf{x}'}\frac{\zeta_t'}{R}\left[(1+D^2)^{-\frac{1}{2}} - 1 + \tfrac{1}{2}D^2\right]\mathrm{d}\mathbf{x}'. \tag{9}$$

Here, $D = (\eta'-\eta)/R$ and $R = |\mathbf{x}'-\mathbf{x}|$. Further, $\eta' = \eta(\mathbf{x}', t)$, $\widetilde{\phi}' = \widetilde{\phi}(\mathbf{x}', t)$, $\zeta_t' = \zeta_t(\mathbf{x}', t)$, $\nabla' = (\partial x_1', \partial x_2')$ etc. The integrals in (9) were integrated numerically by Fructus et al. [9]. The terms expressed by Fourier transform represent a global evaluation of the nonlinear wave field. The remaining terms $\mathcal{R}_2$ obtained in (9) represent contributions computed by local integration.

The purpose of the present paper is to express also $\mathcal{R}_2$ in terms of Fourier series expansions. This has the advantage that only FFTs of the wave field are required to obtain the fully nonlinear motion and is a simplification of

the computational strategy. The formulas provide alternative expressions and computational strategy compared to the direct numerical integration of $\mathcal{R}_2$. Through three-dimensional calculations we illustrate the magnitude of the various terms in (7)–(9) for a sine wave and a model irregular wave field.

Once the potential $\widetilde{\phi}$ is obtained, the orbital velocity at the surface is readily obtained by

$$(u_1, u_2) = \nabla\widetilde{\phi} - \frac{\zeta_t + \nabla\eta\cdot\nabla\widetilde{\phi}}{(1+|\nabla\eta|^2)}\nabla\eta, \tag{10}$$

where ∇ denotes the horizontal gradient.

3 Fourier transform of the integral equation

3.1 The right-hand side of the integral equation (6)

The integral equation has two integral terms. We consider first the integral $(1/2\pi)\int_{\mathbf{x}'}(1/r)\zeta_t'\mathrm{d}\mathbf{x}'$ on the right-hand side of (6). The aim is to express this term by a sum of Fourier transforms. We note that $1/r = (1/R)(1+D^2)^{-\frac{1}{2}}$ where $R = |\mathbf{x}-\mathbf{x}'|$ and $D^2 = (\eta-\eta')^2/R^2$. Making use of Taylor series expansion ($D^2 < 1$) we obtain

$$\frac{1}{r} = \frac{1}{R} - \frac{(\eta-\eta')^2}{2\,R^3} + \frac{3(\eta-\eta')^4}{2^2\cdot 2!\,R^5} - \frac{3\cdot 5(\eta-\eta')^6}{2^3\cdot 3!\,R^7} + \cdots \tag{11}$$

We then use that $1/R = 2\pi\mathcal{F}^{-1}(\mathrm{e}^{-\mathrm{i}\mathbf{k}\cdot\mathbf{x}'}/k)$ (where $\mathcal{F}^{-1}$ denotes inverse Fourier transform). By differentiation we obtain

$$\frac{1}{R^{2n+1}} = \frac{\mathcal{F}^{-1}[2\pi\mathrm{e}^{-\mathrm{i}\mathbf{k}\cdot\mathbf{x}'}(-k^2)^n/k]}{1^2\cdot 3^2\cdot 5^2\cdot\cdots\cdot(2n-1)^2}. \tag{12}$$

This means that

$$\begin{aligned}\frac{1}{2\pi r} &= \mathcal{F}^{-1}\left[\mathrm{e}^{-\mathrm{i}\mathbf{k}\cdot\mathbf{x}'}\left(\frac{1}{k} + \frac{k(\eta-\eta')^2}{2!} + \frac{k^3(\eta-\eta')^4}{4!} + \frac{k^5(\eta-\eta')^6}{6!} + \cdots\right)\right]\\ &= \mathcal{F}^{-1}\left(\sum_{n=0}^{\infty}\sum_{m=0}^{2n}\frac{k^{2n-1}\eta^{2n-m}(-\eta')^m\mathrm{e}^{-\mathrm{i}\mathbf{k}\cdot\mathbf{x}'}}{(2n-m)!\,m!}\right),\end{aligned} \tag{13}$$

where we have used the binominal formula to obtain the latter expression. By carrying out the integration over the $\mathbf{x}'$-variable we obtain

$$\frac{1}{2\pi}\int_{\mathbf{x}'}\zeta_t'(-\eta')^m\mathcal{F}^{-1}[k^{2n-1}\mathrm{e}^{-\mathrm{i}\mathbf{k}\cdot\mathbf{x}'}]\mathrm{d}\mathbf{x}' = \mathcal{F}^{-1}\{k^{2n-1}\mathcal{F}[\zeta_t(-\eta)^m]\}, \tag{14}$$

giving

$$\frac{1}{2\pi}\int_{\mathbf{x}'}\frac{\zeta_t'\mathrm{d}\mathbf{x}'}{r} = \sum_{n=0}^{\infty}\sum_{m=0}^{2n}\frac{\eta^{2n-m}\mathcal{F}^{-1}\{k^{2n-1}\mathcal{F}[\zeta_t(-\eta)^m]\}}{(2n-m)!\,m!} = \sum_{n=0}^{\infty}\Gamma^{(2n+1)}(\zeta_t,\eta). \tag{15}$$

Expressed entirely by moments of the spatial surface elevation, η^{2n-m}, times the inverse Fourier transform, $\mathcal{F}^{-1}\{k^{2n-1}\mathcal{F}[\zeta_t(-\eta)^m]\}$, the sum in (15) gives the fully nonlinear representation of the integral. The contributions involving linear, cubic, quintic and products to seventh power read

$$\Gamma^{(1)}(\zeta_t,\eta)=\frac{1}{2\pi}\int\limits_{\mathbf{x}'}\frac{\zeta_t'\mathrm{d}\mathbf{x}'}{R}=\mathcal{F}^{-1}\left[\frac{\mathcal{F}(\zeta_t)}{k}\right], \tag{16}$$

$$\Gamma^{(3)}(\zeta_t,\eta)=\tfrac{1}{2}\eta^2\mathcal{F}^{-1}[k\mathcal{F}(\zeta_t)]-\eta\mathcal{F}^{-1}[k\mathcal{F}(\zeta_t\eta)]+\tfrac{1}{2}\mathcal{F}^{-1}[k\mathcal{F}(\zeta_t\eta^2)], \tag{17}$$

$$\begin{aligned}\Gamma^{(5)}(\zeta_t,\eta)=&\tfrac{1}{24}\eta^4\mathcal{F}^{-1}[k^3\mathcal{F}(\zeta_t)]-\tfrac{1}{6}\eta^3\mathcal{F}^{-1}[k^3\mathcal{F}(\zeta_t\eta)]+\tfrac{1}{4}\eta^2\mathcal{F}^{-1}[k^3\mathcal{F}(\zeta_t\eta^2)]\\&-\tfrac{1}{6}\eta\mathcal{F}^{-1}[k^3\mathcal{F}(\zeta_t\eta^3)]+\tfrac{1}{24}\mathcal{F}^{-1}[k^3\mathcal{F}(\zeta_t\eta^4)],\end{aligned} \tag{18}$$

$$\begin{aligned}\Gamma^{(7)}(\zeta_t,\eta)=&\tfrac{1}{6!}\eta^6\mathcal{F}^{-1}[k^5\mathcal{F}(\zeta_t)]-\tfrac{1}{5!}\eta^5\mathcal{F}^{-1}[k^5\mathcal{F}(\zeta_t\eta)]+\tfrac{1}{4!2!}\eta^4\mathcal{F}^{-1}[k^5\mathcal{F}(\zeta_t\eta^2)]\\&-\tfrac{1}{3!3!}\eta^3\mathcal{F}^{-1}[k^5\mathcal{F}(\zeta_t\eta^3)]+\tfrac{1}{2!4!}\eta^2\mathcal{F}^{-1}[k^5\mathcal{F}(\zeta_t\eta^4)]-\tfrac{1}{5!}\eta\mathcal{F}^{-1}[k^5\mathcal{F}(\zeta_t\eta^5)]\\&+\tfrac{1}{6!}\eta\mathcal{F}^{-1}[k^5\mathcal{F}(\zeta_t\eta^6)],\end{aligned} \tag{19}$$

and so on. Expression (16) gives the linear contribution of the full integral, Eq. 17 the cubic contribution (given also in (8)), the sum of expressions in (18) the quintic contribution, expression (19) contains products of seventh power, and so on. (Note that $\Gamma^{(1)}(\zeta_t,\eta)$ is independent of η.)

3.2 The left-hand side of (6)

Consider the integral

$$\Phi(\widetilde{\phi},\eta)=\frac{1}{2\pi}\int\limits_{\mathbf{x}'}\widetilde{\phi}'\left(1+|\nabla'\eta'|^2\right)^{\frac{1}{2}}\frac{\partial}{\partial n'}\frac{1}{r}\mathrm{d}\mathbf{x}', \tag{20}$$

where the integrand may be rewritten as

$$\left(1+|\nabla'\eta'|^2\right)^{\frac{1}{2}}\frac{\partial}{\partial n'}\frac{1}{r}=(1+D^2)^{-\frac{3}{2}}\nabla'\cdot\left[(\eta'-\eta)\nabla'\frac{1}{R}\right]. \tag{21}$$

We expand $(1+D^2)^{-3/2}$ in Taylor series ($D^2<1$) and use that $\nabla'\cdot[(\eta'-\eta)\nabla'(1/R)]=\nabla'\eta'\cdot\nabla'(1/R)-(\eta-\eta')(1/R^3)$. By taking the gradient of (12) we obtain

$$\frac{1}{R^{2n}}\nabla'\frac{1}{R}=\frac{1}{2n+1}\nabla'\frac{1}{R^{2n+1}}=\frac{(2n+1)\mathcal{F}^{-1}[2\pi\mathrm{e}^{-\mathrm{i}\mathbf{k}\cdot\mathbf{x}'}(-k^2)^n(-\mathrm{i}\mathbf{k})/k]}{1^2\cdot3^2\cdot5^2\cdots(2n+1)^2}, \tag{22}$$

and

$$\frac{(-1)^n}{2\pi}\frac{1\cdot3\cdot5\cdots(2n-1)\cdot(2n+1)^2(\eta-\eta')^{2n}}{2^n\,n!\,R^{2n}}\nabla'\eta'\cdot\nabla'\frac{1}{R}=-\frac{(\eta-\eta')^{2n}\nabla'\eta'\cdot\mathcal{F}^{-1}(\mathrm{e}^{-\mathrm{i}\mathbf{k}\cdot\mathbf{x}'}k^{2n-1}\mathrm{i}\mathbf{k})}{(2n)!}. \tag{23}$$

Using (12) again, we obtain

$$-\frac{(-1)^n}{2\pi}\frac{1\cdot3\cdot5\cdot\cdots\cdot(2n+1)(\eta-\eta')^{2n+1}}{2^n\,n!\,R^{3+2n}}=\frac{(\eta-\eta')^{2n+1}\mathcal{F}^{-1}(\mathrm{e}^{-\mathrm{i}\mathbf{k}\cdot\mathbf{x}'}k^{2n+1})}{(2n+1)!}. \tag{24}$$

By using the binominal formula for $(\eta-\eta')^{2n+1}$ and carrying out the integration over the $\mathbf{x}'$-variable, the function $\Phi(\widetilde{\phi},\eta)$ in (20) becomes

$$\Phi(\widetilde{\phi},\eta)=\sum_{n=0}^{\infty}\Phi^{(2n+2)}(\widetilde{\phi},\eta) \tag{25}$$

where

$$\Phi^{(2n+2)}(\widetilde{\phi},\eta)=\sum_{m=0}^{2n}\frac{\eta^{2n-m}\mathcal{F}^{-1}\{k^{2n-1}\mathrm{i}\mathbf{k}\cdot\mathcal{F}[\widetilde{\phi}(-\eta)^m\nabla\eta]\}}{(2n-m)!m!}-\sum_{m=0}^{2n+1}\frac{\eta^{2n+1-m}\mathcal{F}^{-1}\{k^{2n+1}\mathcal{F}[\widetilde{\phi}(-\eta)^m]\}}{(2n+1-m)!m!}, \tag{26}$$

and $n \geq 0$. The sums in (26) involve moments of η times the inverse Fourier transform of: the wavenumber times the Fourier transform of products between $\widetilde{\phi}$, η^m and $\nabla\eta$. Contributions to the integral involving quadratic terms, products of fourth power and sixth power, read

$$\Phi^{(2)}(\widetilde{\phi},\eta) = \mathcal{F}^{-1}\left[\frac{\mathrm{i}\mathbf{k}}{k}\cdot\mathcal{F}(\widetilde{\phi}\nabla\eta)\right] - \eta\mathcal{F}^{-1}[k\mathcal{F}(\widetilde{\phi})] + \mathcal{F}^{-1}[k\mathcal{F}(\widetilde{\phi}\eta)], \tag{27}$$

$$\begin{aligned}\Phi^{(4)}(\widetilde{\phi},\eta) = {} & \frac{1}{2}\eta^2\mathcal{F}^{-1}[k\mathrm{i}\mathbf{k}\cdot\mathcal{F}(\widetilde{\phi}\nabla\eta)] - \eta\mathcal{F}^{-1}[k\mathrm{i}\mathbf{k}\cdot\mathcal{F}(\widetilde{\phi}\eta\nabla\eta)] + \frac{1}{2}\mathcal{F}^{-1}[k\mathrm{i}\mathbf{k}\cdot\mathcal{F}(\widetilde{\phi}\eta^2\nabla\eta)] \\ & - \frac{1}{6}\eta^3\mathcal{F}^{-1}[k^3\mathcal{F}(\widetilde{\phi})] + \frac{1}{2}\eta^2\mathcal{F}^{-1}[k^3\mathcal{F}(\widetilde{\phi}\eta)] - \frac{1}{2}\eta\mathcal{F}^{-1}[k^3\mathcal{F}(\widetilde{\phi}\eta^2)] + \frac{1}{6}\mathcal{F}^{-1}[k^3\mathcal{F}(\widetilde{\phi}\eta^3)],\end{aligned} \tag{28}$$

$$\begin{aligned}\Phi^{(6)}(\widetilde{\phi},\eta) = {} & \frac{1}{24}\eta^4\mathcal{F}^{-1}[k^3\mathrm{i}\mathbf{k}\cdot\mathcal{F}(\widetilde{\phi}\nabla\eta)] - \frac{1}{6}\eta^3\mathcal{F}^{-1}[k^3\mathrm{i}\mathbf{k}\cdot\mathcal{F}(\widetilde{\phi}\eta\nabla\eta)] \\ & + \frac{1}{4}\eta^2\mathcal{F}^{-1}[k^3\mathrm{i}\mathbf{k}\cdot\mathcal{F}(\widetilde{\phi}\eta^2\nabla\eta)] - \frac{1}{6}\eta\mathcal{F}^{-1}[k^3\mathrm{i}\mathbf{k}\cdot\mathcal{F}(\widetilde{\phi}\eta^3\nabla\eta)] + \frac{1}{24}\mathcal{F}^{-1}[k^3\mathrm{i}\mathbf{k}\cdot\mathcal{F}(\widetilde{\phi}\eta^4\nabla\eta)] \\ & - \frac{1}{120}\eta^5\mathcal{F}^{-1}[k^5\mathcal{F}(\widetilde{\phi})] + \frac{1}{24}\eta^4\mathcal{F}^{-1}[k^5\mathcal{F}(\widetilde{\phi}\eta)] - \frac{1}{12}\eta^3\mathcal{F}^{-1}[k^5\mathcal{F}(\widetilde{\phi}\eta^2)] \\ & + \frac{1}{12}\eta^2\mathcal{F}^{-1}[k^5\mathcal{F}(\widetilde{\phi}\eta^3)] - \frac{1}{24}\eta\mathcal{F}^{-1}[k^5\mathcal{F}(\widetilde{\phi}\eta^4)] + \frac{1}{120}\mathcal{F}^{-1}[k^5\mathcal{F}(\widetilde{\phi}\eta^5)],\end{aligned} \tag{29}$$

and so on. Using partial integration we note that $\Phi^{(2)}(\widetilde{\phi},\eta)$ equals the quadratic contribution in (7).

3.3 Effect of a finite depth

The effect of a finite water depth is accounted for replacing the Green function by $1/r+1/r_1$ where the latter accounts for an image with respect to the bottom boundary located at $y=-h$. Thus, $1/r_1 = [R^2+(\eta'+\eta+2h)^2]^{-\frac{1}{2}} = (1+\Delta^2)^{-\frac{1}{2}}/R_1$, where $R_1^2 = R^2+4h^2$ and $\Delta^2 = (\eta'+\eta)(\eta'+\eta+4h)/R_1^2$. We show in the Appendix that

$$\frac{1}{2\pi}\int\limits_{\mathbf{x}'}\frac{\zeta_t}{r_1}\mathrm{d}\mathbf{x}' = \sum_{n=0}^{\infty}\Upsilon^{(n+1)}(\zeta_t,\eta), \tag{30}$$

where

$$\Upsilon^{(n+1)}(\zeta_t,\eta) = \frac{(-1)^n\sum_{m=0}^{n}\sum_{q=0}^{n}\binom{n}{m}\binom{n}{q}\eta^{n-m}(\eta+4h)^{n-q}\mathcal{F}^{-1}[\mathrm{e}^{-2kh}p_{n-1}(2kh)\mathcal{F}(\zeta_t\eta^{m+q})]}{2^n n!(2h)^{2n-1}}. \tag{31}$$

We note that $\Upsilon^{(1)}(\zeta_t) = \mathcal{F}^{-1}[\mathrm{e}^{-2kh}\mathcal{F}(\zeta_t)/k]$.

The effect of the horizontal bottom of the fluid layer means that the dipole $(\partial/\partial n)(1/r)$ is replaced by $(\partial/\partial n)(1/r+1/r_1)$ in the integral equation. This results in a new term on the left-hand side of the equation similar to the one in (20) with integrand ($\mathbf{R}=\mathbf{x}'-\mathbf{x}$)

$$\left(1+|\nabla'\eta'|^2\right)^{\frac{1}{2}}\frac{\partial}{\partial n'}\frac{1}{r_1} = -\frac{y'+y+2h-\nabla'\eta'\cdot\mathbf{R}}{r_1^3}. \tag{32}$$

In the Appendix we show that

$$\frac{1}{2\pi}\int\limits_{\mathbf{x}'}\widetilde{\phi}'\frac{\partial}{\partial n'}\frac{1}{r_1}\mathrm{d}S = \Psi^{(1)}(\widetilde{\phi}) + \sum_{n=0}^{\infty}\Psi^{(n+2)}(\widetilde{\phi},\eta), \tag{33}$$

where $\Psi^{(1)}(\widetilde{\phi},\eta) = -\mathcal{F}^{-1}[\mathrm{e}^{-2kh}\mathcal{F}(\widetilde{\phi})]$, and, for $n \geq 0$,

$$\begin{aligned}\Psi^{(n+2)}(\widetilde{\phi},\eta) = &\sum_{m=0}^{n+1}\sum_{q=0}^{n}\binom{n+1}{m}\binom{n}{q}\eta^{n+1-m}(\eta+4h)^{n-q}\frac{(-1)^{n+1}\mathcal{F}^{-1}[\mathrm{e}^{-2kh}p_n(2kh)\mathcal{F}(\widetilde{\phi}\eta^{m+q})]}{2^n n!\ (2h)^{2n+1}}\\ &+2h\sum_{m=0}^{n+1}\sum_{q=0}^{n+1}\binom{n+1}{m}\binom{n+1}{q}\eta^{n+1-m}(\eta+4h)^{n+1-q}\frac{(-1)^{n}\mathcal{F}^{-1}[\mathrm{e}^{-2kh}p_{n+1}(2kh)\mathcal{F}(\widetilde{\phi}\eta^{m+q})]}{2^{n+1}(n+1)!\ (2h)^{2n+3}}\\ &+\sum_{m=0}^{n}\sum_{q=0}^{n}\binom{n}{m}\binom{n}{q}\eta^{n-m}(\eta+4h)^{n-q}\frac{(-1)^{n}\mathcal{F}^{-1}[\mathrm{e}^{-2kh}p_{n-1}(2kh)\,\mathrm{i}\mathbf{k}\cdot\mathcal{F}(\widetilde{\phi}\eta^{m+q}\nabla\eta)]}{2^n n!(2h)^{2n-1}},\end{aligned} \tag{34}$$

where the polynomials $p_n(2kh)$ are defined in the Appendix.

4 Solution of the integral equation

4.1 Infinite water depth

The integral equation becomes, for $h = \infty$,

$$\widetilde{\phi} + \Phi^{(2)}(\widetilde{\phi},\eta) + \Phi^{(4)}(\widetilde{\phi},\eta) + \cdots = \mathcal{F}^{-1}\left[\frac{\mathcal{F}(\zeta_t)}{k}\right] + \Gamma^{(3)}(\zeta_t,\eta) + \Gamma^{(5)}(\zeta_t,\eta) + \cdots \tag{35}$$

where $\Gamma^{(2n+1)}(\zeta_t,\eta)$ and $\Phi^{(2n)}(\widetilde{\phi},\eta)$, $n = 1, 2, \ldots$, are given in (15) and (26), respectively. Let us introduce

$$\widetilde{\phi}_{(0,1)} = \mathcal{F}^{-1}\left[\frac{\mathcal{F}(\zeta_t)}{k}\right] \tag{36}$$

and obtain recursively

$$\widetilde{\phi}_{(0,2n+1)} = \widetilde{\phi}_{(0,2n-1)} + \Gamma^{(2n+1)}(\zeta_t,\eta), \quad n = 1, 2, \ldots, \tag{37}$$

the sequence $\{\widetilde{\phi}_{(0,2n+1)}\}$, $n = 0, 1, \ldots$, represents increasingly improved approximations to the right-hand side of (35).

Improved approximations to the solution of (35) are obtained. With $\widetilde{\phi}_{(0,3)}$ given in (37) with $n = 1$, the cubic approximation is obtained by solving iteratively the equation

$$\widetilde{\phi}_{(m,3)} = \widetilde{\phi}_{(0,3)} - \Phi^{(2)}(\widetilde{\phi}_{(m-1,3)},\eta), \tag{38}$$

for $m = 1, 2, \ldots$, until convergence is obtained. Only very few iterations are required in practice. Equation 38 corresponds to Eq. 7 with $\mathcal{R}_1$ expressed by (8) and $\mathcal{R}_2$ in (8) put to zero.

The quintic approximation to (35) is obtained by solving iteratively

$$\widetilde{\phi}_{(m,5)} = \widetilde{\phi}_{(0,5)} - \Phi^{(2)}(\widetilde{\phi}_{(m-1,5)},\eta) - \Phi^{(4)}(\widetilde{\phi}_{(m-1,5)},\eta), \tag{39}$$

for $m = 1, 2, \ldots$, with $\widetilde{\phi}_{(0,5)}$ given by (37) with $n = 2$. Likewise, the seventh-order approximation to (35) is obtained by solving iteratively

$$\widetilde{\phi}_{(m,7)} = \widetilde{\phi}_{(0,7)} - \Phi^{(2)}(\widetilde{\phi}_{(m-1,7)},\eta) - \Phi^{(4)}(\widetilde{\phi}_{(m-1,7)},\eta) - \Phi^{(6)}(\widetilde{\phi}_{(m-1,7)},\eta), \tag{40}$$

for $m = 1, 2, \ldots$, with $\widetilde{\phi}_{(0,7)}$ given by (37) with $n = 3$. Similarly, higher-order approximations to (35) yield higher-order solutions to the integral equation.

4.2 Finite depth

For finite water depth the integral equation becomes

$$\mathcal{F}^{-1}[(1-\mathrm{e}^{-2kh})\mathcal{F}(\widetilde{\phi})] + \Phi^{(2)}(\widetilde{\phi},\eta) + \Phi^{(4)}(\widetilde{\phi},\eta) + \cdots + \Psi^{(2)}(\widetilde{\phi},\eta) + \Psi^{(3)}(\widetilde{\phi},\eta)$$
$$+ \Psi^{(4)}(\widetilde{\phi},\eta) + \Psi^{(5)}(\widetilde{\phi},\eta) + \cdots = \mathcal{F}^{-1}\left[\frac{(1+\mathrm{e}^{-2kh})\mathcal{F}(\zeta_t)}{k}\right] + \Gamma^{(3)}(\zeta_t,\eta) + \Gamma^{(5)}(\zeta_t,\eta)$$
$$+ \cdots + \Upsilon^{(2)}(\zeta_t,\eta) + \Upsilon^{(3)}(\zeta_t,\eta) + \Upsilon^{(4)}(\zeta_t,\eta) + \Upsilon^{(5)}(\zeta_t,\eta) + \cdots \tag{41}$$

The functions correcting for the effect of a finite depth include $\Psi^{(n)}(\widetilde{\phi},\eta)$, $n = 1, 2, \ldots$, defined in (66), and $\Upsilon^{(n)}(\zeta_t,\eta)$, $n = 1, 2, \ldots$, defined in (59). As before, $\Gamma^{(2n+1)}(\zeta_t,\eta)$ and $\Phi^{(2n)}(\widetilde{\phi},\eta)$, $n = 1, 2, \ldots$, are given in (15) and (26), respectively.

Similarly as for infinite depth we define $\widetilde{\phi}_{(0,1,h)}$ by

$$\mathcal{F}^{-1}[(1-\mathrm{e}^{-2kh})\mathcal{F}(\widetilde{\phi}_{(0,1,h)})] = \mathcal{F}^{-1}\left[\frac{(1+\mathrm{e}^{-2kh})\mathcal{F}(\zeta_t)}{k}\right]. \tag{42}$$

We then define successively $\widetilde{\phi}_{(0,2n+1,h)}$, $n = 1, 2, \ldots$ by

$$\mathcal{F}^{-1}[(1-\mathrm{e}^{-2kh})\mathcal{F}(\widetilde{\phi}_{(0,2n+1,h)})]$$
$$= \mathcal{F}^{-1}[(1-\mathrm{e}^{-2kh})\mathcal{F}(\widetilde{\phi}_{(0,2n-1,h)})] + \Gamma^{(2n+1)}(\zeta_t,\eta) + \Upsilon^{(2n)}(\zeta_t,\eta) + \Upsilon^{(2n+1)}(\zeta_t,\eta), \tag{43}$$

which approximates the right-hand side of (41).

Successive approximations to the integral equation (41) are then obtained. The cubic approximation is obtained by solving iteratively

$$\mathcal{F}^{-1}[(1-\mathrm{e}^{-2kh})\mathcal{F}(\widetilde{\phi}_{(m,3,h)})] = \mathcal{F}^{-1}[(1-\mathrm{e}^{-2kh})\mathcal{F}(\widetilde{\phi}_{(0,3,h)})]$$
$$-\Phi^{(2)}(\widetilde{\phi}_{(m-1,3,h)},\eta) - \Psi^{(2)}(\widetilde{\phi}_{(m-1,3,h)},\eta) - \Psi^{(3)}(\widetilde{\phi}_{(m-1,3,h)},\eta), \tag{44}$$

for $m = 1, 2, \ldots$ Similarly, the quintic approximation is obtained by

$$\mathcal{F}^{-1}[(1-\mathrm{e}^{-2kh})\mathcal{F}(\widetilde{\phi}_{(m,5,h)})] = \mathcal{F}^{-1}[(1-\mathrm{e}^{-2kh})\mathcal{F}(\widetilde{\phi}_{(0,5,h)})]$$
$$-\Phi^{(2)}(\widetilde{\phi}_{(m-1,5,h)},\eta) - \Phi^{(4)}(\widetilde{\phi}_{(m-1,5,h)},\eta)$$
$$-\Psi^{(2)}(\widetilde{\phi}_{(m-1,5,h)},\eta) - \Psi^{(3)}(\widetilde{\phi}_{(m-1,5,h)},\eta) - \Psi^{(4)}(\widetilde{\phi}_{(m-1,5,h)},\eta)$$
$$-\Psi^{(5)}(\widetilde{\phi}_{(m-1,5,h)},\eta), \tag{45}$$

$m = 1, 2, \ldots$ Higher-order approximations to the integral equation (41) are obtained similarly.

5 Numerical examples

5.1 Computations for a sine-wave

We assume for simplicity that the water depth is infinite and that there is no current. We consider a periodic sine-wave and assume that $\eta_t = 0.3\sin x_1$ and $\eta = 0.3\cos x_1$ for $0 < x_1, x_2 < 2\pi$ (a very strong wave). There are 64 nodes in each horizontal direction. The first five terms on the right-hand side of the integral equation are visualized in Figs. 1a–e. The computations show that $\Gamma^{(2n+1)}$ behave like $\delta_{2n+1}\sin x_1$, $n = 0, 1, 2, \ldots$, where the coefficients have alternating sign. They are, roughly, $\delta_1 \sim 3\times10^{-1}$, $\delta_3 \sim -7\times10^{-3}$, $\delta_5 \sim 3\times10^{-4}$, $\delta_7 \sim -1.7\times10^{-5}$ and $\delta_9 \sim 1\times10^{-6}$ (in this example). Ratios are: $|\delta_1/\delta_3| \sim 43$, $|\delta_3/\delta_5| \sim 23$, $|\delta_5/\delta_7| \sim 18$ and $|\delta_7/\delta_9| \sim 17$. The effect of truncation may be estimated by the next term of the expansion that is left out: A relative error of 1/1,000 is obtained by including terms up to $\Gamma^{(3)}$. The relative error becomes 5×10^{-5} by including terms up to $\Gamma^{(5)}$, and 3×10^{-6} by including terms up to $\Gamma^{(7)}$. Figure 1f illustrates that the sum $\Gamma^{(5)} + \Gamma^{(7)} + \Gamma^{(9)}$ and the integral

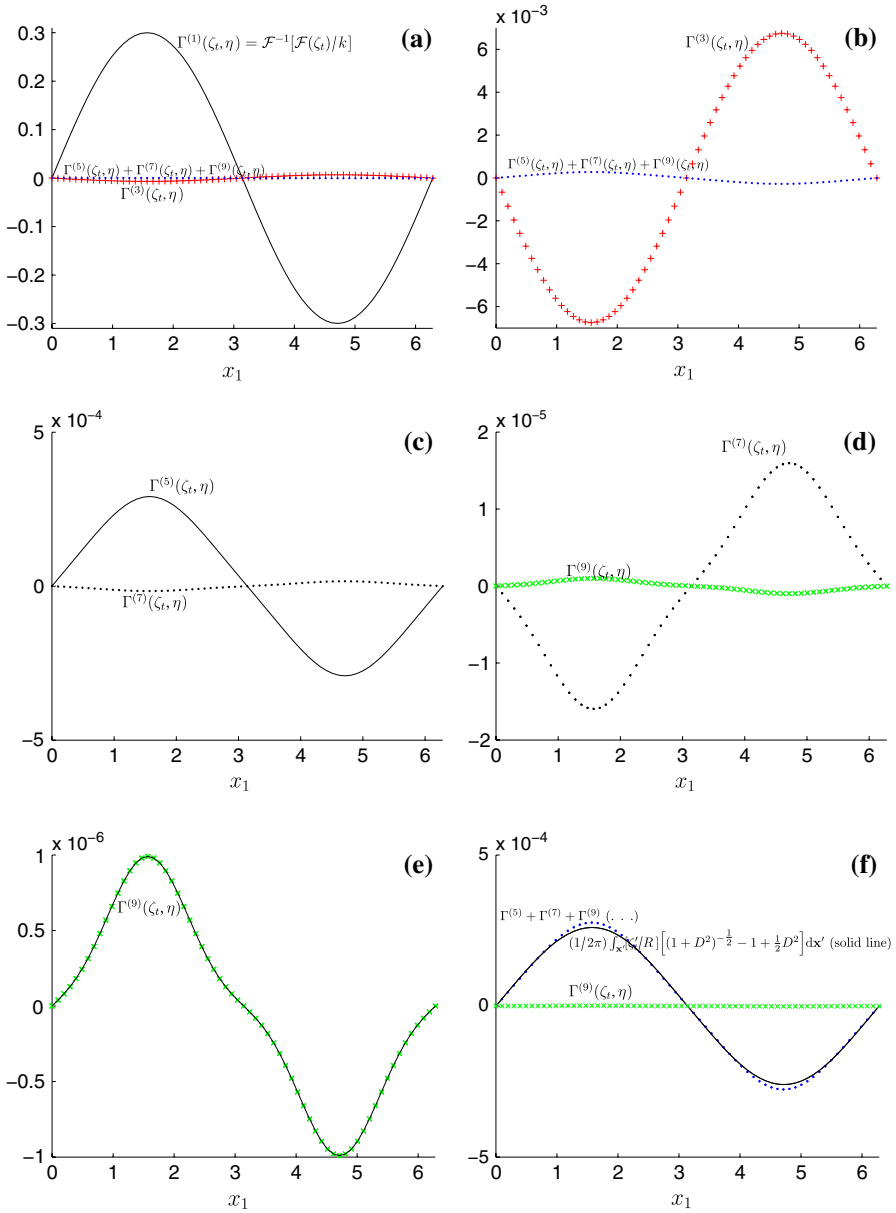

Fig. 1 **a** $\Gamma^{(1)}(\zeta_t,\eta)=\mathcal{F}^{-1}[\mathcal{F}(\zeta_t)/k]$ (*solid line*), $\Gamma^{(3)}(\zeta_t,\eta)$ (+++) and $\Gamma^{(5)}(\zeta_t,\eta)+\Gamma^{(7)}(\zeta_t,\eta)+\Gamma^{(9)}(\zeta_t,\eta)$ (...). **b** $\Gamma^{(3)}(\zeta_t,\eta)$ (+++) and $\Gamma^{(5)}(\zeta_t,\eta)+\Gamma^{(7)}(\zeta_t,\eta)+\Gamma^{(9)}(\zeta_t,\eta)$ (...). **c** $\Gamma^{(5)}(\zeta_t,\eta)$ (*solid line*) and $\Gamma^{(7)}(\zeta_t,\eta)$ (...). **d** $\Gamma^{(7)}(\zeta_t,\eta)$ (...) and $\Gamma^{(9)}(\zeta_t,\eta)$ ($\times\times\times$). **e** $\Gamma^{(9)}(\zeta_t,\eta)$ (*solid line*) and ($\times\times\times$). **f** $\Gamma^{(5)}(\zeta_t,\eta)+\Gamma^{(7)}(\zeta_t,\eta)+\Gamma^{(9)}(\zeta_t,\eta)$ (...), $(1/2\pi)\int_{\mathbf{x}'}[\zeta_t'/R]\left[(1+D^2)^{-\frac{1}{2}}-1+\frac{1}{2}D^2\right]\mathrm{d}\mathbf{x}'$ (*solid line*) and $\Gamma^{(9)}(\zeta_t,\eta)$ ($\times\times\times$). Input wave field: $\eta_t=0.3\sin x_1$, $\eta=0.3\cos x_1$. Basin: $0<x_1,x_2<2\pi$. 64×64 resolution

$(1/2\pi)\int_{\mathbf{x}'}\frac{\zeta_t'}{R}\left[(1+D^2)^{-\frac{1}{2}}-1+\frac{1}{2}D^2\right]\mathrm{d}\mathbf{x}'$ in (9) are very close, where the former is more accurate than the latter. The estimate of the integral becomes improved by increasing the resolution.

The contributions to the integral on the left-hand side are illustrated by computing $-\Phi^{(2n+2)}(\phi_0,\eta)$ (with a resolution of 50 by 50) with the potential given by $\phi_0=\mathcal{F}^{-1}[\mathcal{F}(\eta_t)/k]$. While the individual contributions to $\Phi^{(2)}$ are not small, an exact cancellation is taking place for this particular choice of ϕ_0 and η, giving that $\Phi^{(2)}(\phi_0,\eta)=0$. Computations in Figs. 2a–c show that $-\Phi^{(2n+2)}(\phi_0,\eta)$ behave like $\delta_{2n+2}\sin 2x_1$, $n=1,2,\ldots$, i.e., a double oscillation,

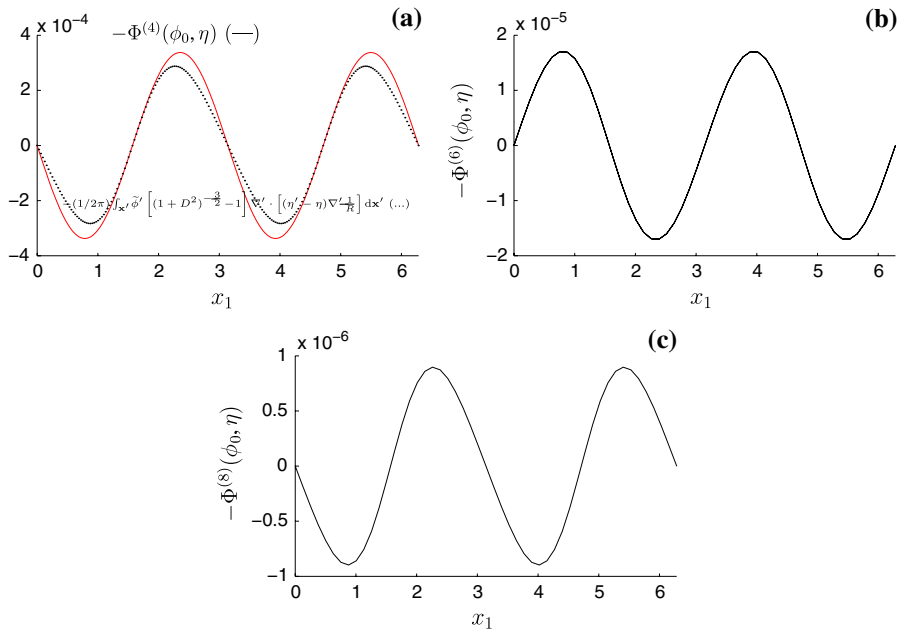

Fig. 2 **a** $-\Phi^{(4)}(\phi_0,\eta)$ (*solid line*) and $-(1/2\pi)\int_{\mathbf{x}'}\widetilde{\phi}'\left[(1+D^2)^{-\frac{3}{2}}-1\right]\nabla'\cdot\left[(\eta'-\eta)\nabla'\frac{1}{R}\right]\mathrm{d}\mathbf{x}'$ (...) (resolution 50×50), **b** $-\Phi^{(6)}(\phi_0,\eta)$ (resolution 50×50 and 200×200), **c** $-\Phi^{(8)}(\phi_0,\eta)$ (resolution 50×50). Input wave field: $\eta_t=0.3\sin x_1, \eta=0.3\cos x_1$. $\phi_0=\mathcal{F}^{-1}[\mathcal{F}(\eta_t)/k]$. Basin: $0<x_1,x_2<2\pi$

where the coefficients have alternating sign. The coefficients are, roughly, $\delta_4\sim-3.5\times10^{-4}$, $\delta_6\sim1.7\times10^{-5}$ and $\delta_8\sim-0.85\times10^{-6}$. The computations show that δ_4 on the right-hand side and δ_5 on the left-hand side are of same magnitude, and similarly for δ_6 and δ_7 (both of magnitude 1.7×10^{-5}), and similarly for δ_8 and δ_9 (both of magnitude 1×10^{-6}). Figure 2a shows that the integral $-(1/2\pi)\int_{\mathbf{x}'}\widetilde{\phi}'\left[(1+D^2)^{-\frac{3}{2}}-1\right]\nabla'\cdot\left[(\eta'-\eta)\nabla'\frac{1}{R}\right]\mathrm{d}\mathbf{x}'$ (with $\widetilde{\phi}=\phi_0$) in (9) and $-\Phi^{(4)}(\phi_0,\eta)$ are relatively close, where evaluation of the latter is more accurate than the former. Improved resolution improves the integral.

Working with the truncation (39), i.e., the quintic approximation to the full integral equation, implies a relative error of 5×10^{-5} with an input wave field given by $\eta_t=0.3\sin x_1$, $\eta=0.3\cos x_1$. Similarly, working with (40), i.e., a seventh-order approximation, means a relative error of 3×10^{-6} (for the same wave field).

5.2 Swath of an irregular wave field

With relevance to the GOTEX experiment [4,5] we consider a model irregular wave field. The instantaneous surface elevation is obtained from a directional JONSWAP spectrum in deep water ($h=\infty$) with $\gamma=3.3$ and $T_p=10$ s. The directionality is given by $D(\alpha)=(1/\beta)\cos^2(\pi\alpha/2\beta)$ for $|\alpha|\le\beta$ ($D=0$ elsewhere) with $\beta=0.7$. The elevation is represented by $\eta(\mathbf{x},t)=\sum_{m=-M/2,n=-N/2}^{M/2-1,N/2-1}A_{mn}\cos\chi_{mn}$ where $\chi_{mn}=\mathbf{k}_{mn}\cdot\mathbf{x}-\omega_{mn}t+\theta_{mn}$, $|A_{mn}|$ is obtained from the spectrum, the argument from random numbers between 0 and 2π, $\mathbf{k}_{mn}=|\mathbf{k}_{mn}|\mathrm{e}^{\mathrm{i}\alpha_{mn}}$ and $M=N=64$. For illustrative purposes we assume that the time derivative is represented by $\eta_t(\mathbf{x},t)=\sum_{m=-M/2,n=-N/2}^{M/2-1,N/2-1}A_{mn}\omega_{mn}\sin\chi_{mn}$. The elevation and its temporal and spatial derivatives are evaluated over a truncated area 2,000 m long and 200 m wide with a resolution of $\Delta x_1=\Delta x_2=2$ m. The slope along the x_1-axis, the main direction of propagation, varies in the range between -0.3 and 0.3 and is a fairly strong sea (Fig. 3a). There is no current.

Calculations of $\Gamma^{(1)}$, $\Gamma^{(3)}$, $\Gamma^{(5)}$ and $\Gamma^{(7)}$ presented in Fig. 3 show a magnitude of the former of about 60 (m^2/s). $\Gamma^{(3)}$ has a magnitude of about 1.6 (m^2/s), $\Gamma^{(5)}$ about 0.1 (m^2/s) and $\Gamma^{(7)}$ about 0.018 (m^2/s). This implies relative ratios of $\Gamma^{(1)}/\Gamma^{(3)}\simeq38$, $\Gamma^{(3)}/\Gamma^{(5)}\simeq16$ and $\Gamma^{(5)}/\Gamma^{(7)}\simeq5$. Calculation of $\Phi^{(2)}(\phi_0,\eta)$ (with $\phi_0=\mathcal{F}^{-1}[\mathcal{F}(\eta_t)/k]$) shows

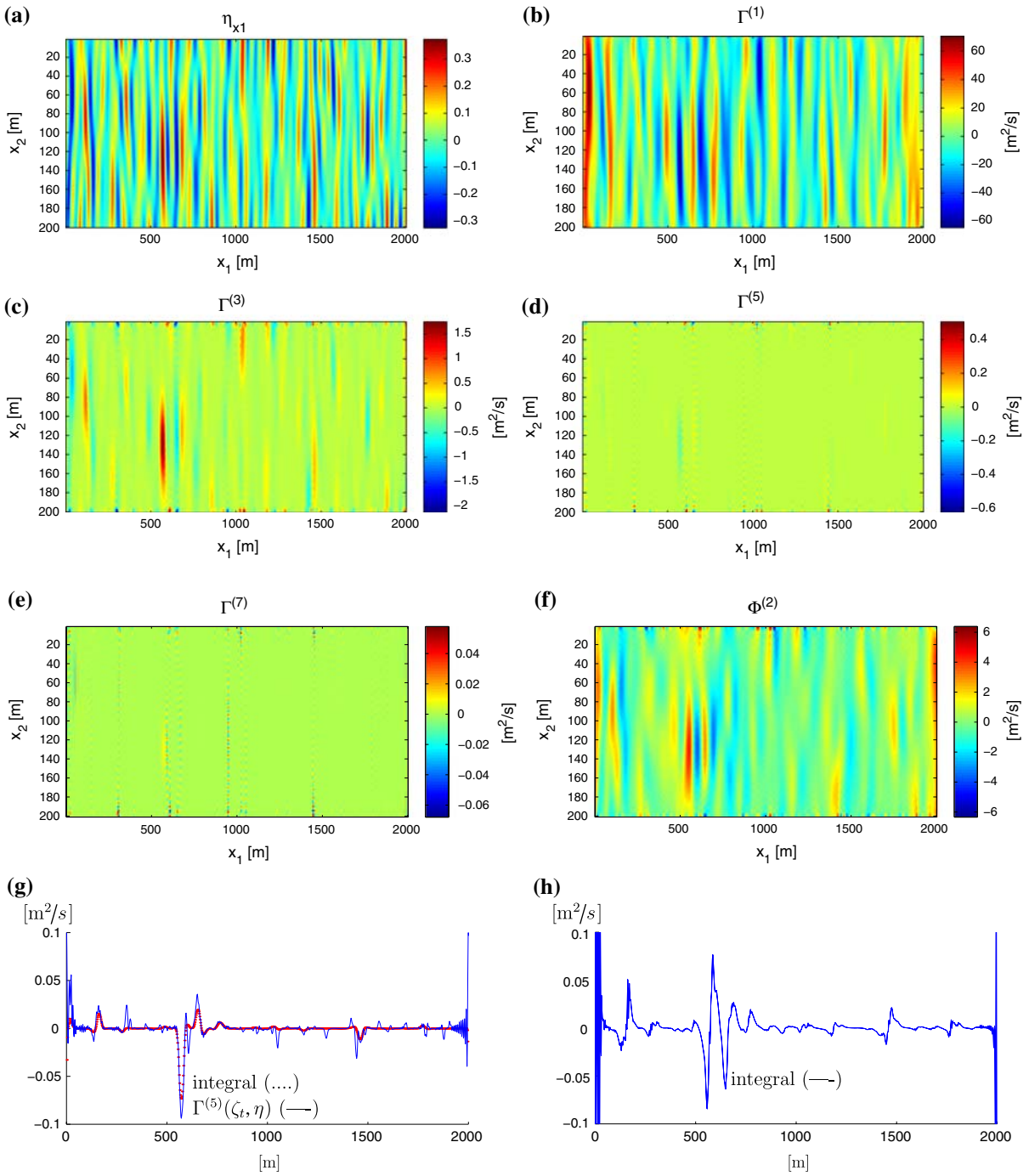

Fig. 3 **a** Wave slope η_{x_1} of irregular sea for $0 < x_1 < 2,000\,\text{m}$, $0 < x_2 < 200\,\text{m}$; **b** $\Gamma^{(1)}(\zeta_t, \eta)$; **c** $\Gamma^{(3)}(\zeta_t, \eta)$; **d** $\Gamma^{(5)}(\zeta_t, \eta)$; **e** $\Gamma^{(7)}(\zeta_t, \eta)$; **f** $\Phi^{(2)}(\phi_0, \eta)$; **g** $\Gamma^{(5)}(\zeta_t, \eta)$ (—-) and $(1/2\pi)\int_{\mathbf{x}'} \frac{\zeta_t'}{R}\left[(1+D^2)^{-\frac{1}{2}} - 1 + \frac{1}{2}D^2\right]\mathrm{d}\mathbf{x}'$ (….) along the section with $x_2 = 140$ m; **h** $(1/2\pi)\int_{\mathbf{x}'} \widetilde{\phi}'\left[(1+D^2)^{-\frac{3}{2}} - 1\right]\nabla' \cdot \left[(\eta' - \eta)\nabla' \frac{1}{R}\right]\mathrm{d}\mathbf{x}'$ along the section with $x_2 = 140\,\text{m}$

that this has a magnitude of about 4 (m^2/s) implying a ratio of $\Gamma^{(1)}/\Phi^{(2)} \simeq 15$ (Fig. 3f). The comparison between $\Gamma^{(5)}$ and the integral $(1/2\pi)\int_{\mathbf{x}'} \frac{\zeta_t'}{R}\left[(1+D^2)^{-\frac{1}{2}} - 1 + \frac{1}{2}D^2\right]\mathrm{d}\mathbf{x}'$ in Fig. 3h shows that both are similar (Fig. 3g). Evaluation of the integral $(1/2\pi)\int_{\mathbf{x}'} \widetilde{\phi}'\left[(1+D^2)^{-\frac{3}{2}} - 1\right]\nabla'\cdot\left[(\eta'-\eta)\nabla'\frac{1}{R}\right]\mathrm{d}\mathbf{x}'$ shows that this has magnitude up to 0.08 (m^2/s) (Fig. 3h). The evaluation of $\Phi^{(4)}$ exploded because the Gibbs phenomenon polluted the function in the entire domain. Evaluation of $\Phi^{(4)}$, $\Phi^{(6)}$ and $\Phi^{(8)}$ did not explode for the coarser resolution of 4 m, however. The functions were clearly affected by the Gibbs phenomenon spreading from the boundaries to the entire domain (results not shown).

The computations of the non-periodic swath (Fig. 3) exhibit Gibbs phenomenon along the boundaries. For the leading contributions ($\Gamma^{(1)}$, $\Gamma^{(3)}$, $\Gamma^{(5)}$, $\Phi^{(2)}$), oscillations were found only along the boundaries. For $\Gamma^{(7)}$, the Gibbs phenomenon polluted the function also in the interior of the domain (but this function has a very small amplitude). The Gibbs phenomenon, moreover, caused the evaluation of $\Phi^{(4)}$ to explode for the relatively fine resolution of 2 m (but not for the coarser one). The effect of the Gibbs phenomenon is avoided for periodic wave fields.

6 Concluding remarks

We have discussed the solution of an integral equation obtaining an accurate representation of the wave potential on the free surface given the spatial wave elevation field, η, and its time derivative, η_t. The method is three-dimensional and is useful for application to realistic wave fields in three dimensions where the wave motion may take place along two horizontal variables. Also, the effect of a horizontal current is accounted for in the formulation. The derivations are motivated by practical needs in oceanographic measurements of storm seas obtaining the surface elevation and its time derivative along regions of the free surface. From the wave record it has been a desire, through a postprocessing of the elevation data, to obtain the orbital velocity in strong wave events [4,5]. Purposes include: enhanced interpretation of the database, evaluation of velocities in breaking events and the entire wave field as such, derive statistics of the wave induced velocities, and compare with potential velocity measurements when available. The derivations and computations presented in this paper are made to support these purposes.

The integral equation we have been dealing with is given in Eq. 6. The effect of a current is accounted for on its right-hand side by the term $(1/2\pi)\int_{\mathbf{x}'} \frac{\zeta_t'}{r}\mathrm{d}\mathbf{x}'$ where $\zeta_t = \eta_t + \mathbf{U}\cdot\nabla\eta$. We have derived formulas that express the nonlinear integrals of the equation in terms of sums of Fourier transforms. The expressions imply that the nonlinearity is computed with global contributions. More specifically we deduced that the integral equation becomes, in the case of infinite water depth (see (35)),

$$\widetilde{\phi} + \Phi^{(2)}(\widetilde{\phi},\eta) + \Phi^{(4)}(\widetilde{\phi},\eta) + \cdots = \mathcal{F}^{-1}\left[\mathcal{F}(\zeta_t)/k\right] + \Gamma^{(3)}(\zeta_t,\eta) + \Gamma^{(5)}(\zeta_t,\eta) + \cdots$$

where $\Gamma^{(2n+1)}(\zeta_t,\eta)$ and $\Phi^{(2n)}(\widetilde{\phi},\eta)$, $n = 1, 2, \ldots$, are expressed by Fourier transform and inverse transform; see (15) and (26), respectively. The terms are easy to implement. In the case of a finite, constant water depth the integral equation has more terms accounting for an image with respect to the sea floor; see (41).

The various contributions to the integral equation have been evaluated in two numerical examples. The calculations for a (periodic) sine-wave with $\eta_t = 0.3\sin x_1$ and $\eta = 0.3\cos x_1$ show the following: all terms on the right-hand side contribute to a sine, and, the terms on the left-hand side also contribute to a sine, but with double the wavenumber. Ratios between the Γ's become (in this case): $\Gamma^{(1)}/\Gamma^{(3)} \simeq 43$, $\Gamma^{(3)}/\Gamma^{(5)} \simeq 23$, $\Gamma^{(5)}/\Gamma^{(7)} \simeq 18$ and $\Gamma^{(7)}/\Gamma^{(9)} \simeq 17$. In this particular case $\Phi^{(2)}$ vanishes exactly. For the other Φ's we find: $\Phi^{(2n)} \sim \Gamma^{(2n+1)}$, $n = 2, 3, 5$. The solution is obtained with a relative error of 5×10^{-5} if the quintic approximation is used, including $\Phi^{(2)}$, $\Phi^{(4)}$, $\Gamma^{(3)}$ and $\Gamma^{(5)}$ (in this case).

In the second example a model directional irregular sea obtained from a directional JONSWAP spectrum over a swath 2,000 m long and 200 m wide has wave slope in the range ±0.3 and a resolution in each direction of 2 m. Calculations of the Γ's and Φ's show ratios of (in this case): $\Gamma^{(1)}/\Gamma^{(3)} \simeq 38$, $\Gamma^{(1)}/\Phi^{(2)} \simeq 15$, $\Gamma^{(3)}/\Gamma^{(5)} \simeq 16$ and $\Gamma^{(5)}/\Gamma^{(7)} \simeq 5$. A relatively good comparison between $\Gamma^{(5)}$ and the integral $(1/2\pi)\int_{\mathbf{x}'} \frac{\zeta_t'}{R}\left[(1+D^2)^{-\frac{1}{2}} - 1 + \frac{1}{2}D^2\right]\mathrm{d}\mathbf{x}'$

was found. The integral $(1/2\pi)\int_{\mathbf{x}'}\widetilde{\phi}'\left[(1+D^2)^{-\frac{3}{2}}-1\right]\nabla'\cdot\left[(\eta'-\eta)\nabla'\frac{1}{R}\right]\mathrm{d}\mathbf{x}'$ is comparable to $\Gamma^{(5)}$. The computations of the non-periodic swath exhibited the Gibbs phenomenon along the boundaries, but did not affect the dominant contributions in the inner part of the domain ($\Gamma^{(1)}$, $\Gamma^{(3)}$, $\Gamma^{(5)}$, $\Phi^{(2)}$). For high-order contributions like $\Gamma^{(7)}$, the Gibbs phenomenon was found to significantly pollute the function also in the interior of the swath. Evaluation of $\Phi^{(4)}$ and the higher-order Φ's exploded for the relatively fine resolution of 2 m but not for a coarser resolution of 4 m.

We note that the orbital velocity of the wave field is obtained from Eq. 10 accounting an evaluation at the actual position of the free surface [5].

Appendix: Effect of a finite depth: derivations

The effect of a finite water depth is accounted for by replacing the source (sink) Green function $1/r$ by $1/r+1/r_1$ where the latter accounts for an image with respect to the bottom boundary located at $y=-h$. Thus, $1/r_1=[R^2+(\eta'+\eta+2h)^2]^{-\frac{1}{2}}=(1+\Delta^2)^{-\frac{1}{2}}/R_1$, where $R_1^2=R^2+4h^2$ and $\Delta^2=(\eta'+\eta)(\eta'+\eta+4h)/R_1^2$. A Taylor series expansion in Δ^2 is used.

Repeated differentiations of the relation $1/R_1=\mathcal{F}^{-1}[T(\mathbf{x}')/k]$ with respect to the variable $2h$, where $T(\mathbf{x}')=2\pi\mathrm{e}^{-\mathrm{i}\mathbf{k}\cdot\mathbf{x}'-2kh}$, $k=|\mathbf{k}|$, gives

$$\frac{1\cdot3\cdot5\cdots(2n-1)(2h)^{2n-1}}{R_1^{2n+1}}=\mathcal{F}^{-1}\{T(\mathbf{x}')p_{n-1}(2kh)\},\quad n=1,2,\ldots \tag{46}$$

$$\frac{1}{2hR_1}=\mathcal{F}^{-1}[T(\mathbf{x}')p_{-1}(2kh)],\quad n=-1 \tag{47}$$

where $p_{n-1}(2kh)=\sum_{m=0}^{n-1}\alpha_{n-1,m}(2kh)^m$ are polynomials of degree $n-1$, for $n\geq1$, and $p_{-1}(2kh)=1/(2kh)$. The first few polynomials read (with $2kh=K$):

$$p_{-1}=\frac{1}{K}, \tag{48}$$

$$p_0=1, \tag{49}$$

$$p_1=K+1, \tag{50}$$

$$p_2=K^2+3(K+1), \tag{51}$$

$$p_3=K^3+6K^2+3\cdot5(K+1), \tag{52}$$

$$p_4=K^4+10K^3+45K^2+3\cdot5\cdot7(K+1), \tag{53}$$

$$p_5=K^5+15K^4+105K^3+15\cdot28K^2+3\cdot5\cdot7\cdot9(K+1), \tag{54}$$

$$p_6=K^6+21K^5+210K^4+105\cdot12K^3+105\cdot45K^2+3\cdot5\cdot7\cdot9\cdot11(K+1), \tag{55}$$

etc. Using the Binominal formula for $(\eta'+\eta)^n=\sum_{m=0}^{n}\binom{n}{m}\eta^{n-m}\eta'^m$ and similar for $(\eta'+\eta+4h)^n=\sum_{q=0}^{n}\binom{n}{q}(\eta+4h)^{n-q}\eta'^q$, we obtain

$$\frac{1}{r_1}=\sum_{n=0}^{\infty}\frac{(-1)^n\sum_{m=0}^{n}\sum_{q=0}^{n}\binom{n}{m}\binom{n}{q}\eta'^{m+q}\eta^{n-m}(\eta+4h)^{n-q}\mathcal{F}^{-1}[T(\mathbf{x}')p_{n-1}(2kh)]}{2^n n!(2h)^{2n-1}} \tag{56}$$

By use of

$$\frac{1}{2\pi}\int_{\mathbf{x}'}\zeta_t'\eta'^{m+q}\mathcal{F}^{-1}[T(\mathbf{x}')p_{n-1}(2kh)]\mathrm{d}\mathbf{x}'=\mathcal{F}^{-1}[\mathrm{e}^{-2kh}p_{n-1}(2kh)\mathcal{F}(\zeta_t\eta^{m+q})], \tag{57}$$

the integral becomes

$$\frac{1}{2\pi}\int\limits_{\mathbf{x}'}\frac{\zeta_t}{r_1}\mathrm{d}\mathbf{x}'=\sum_{n=0}^{\infty}\Upsilon^{(n+1)}(\zeta_t,\eta), \tag{58}$$

where

$$\Upsilon^{(n+1)}(\zeta_t,\eta)=\frac{(-1)^n\sum_{m=0}^{n}\sum_{q=0}^{n}\binom{n}{m}\binom{n}{q}\eta^{n-m}(\eta+4h)^{n-q}\mathcal{F}^{-1}[\mathrm{e}^{-2kh}p_{n-1}(2kh)\mathcal{F}(\zeta_t\eta^{m+q})]}{2^n n!(2h)^{2n-1}}. \tag{59}$$

We note that $\Upsilon^{(1)}(\zeta_t)=\mathcal{F}^{-1}[\mathrm{e}^{-2kh}\mathcal{F}(\zeta_t)/k]$.

The effect of the horizontal bottom of the fluid layer means that the dipole $(\partial/\partial n)(1/r)$ is replaced by $(\partial/\partial n)(1/r+1/r_1)$ in the integral equation. This results in a new term on the left-hand side of the equation similar to the one in (20) with integrand ($\mathbf{R}=\mathbf{x}'-\mathbf{x}$)

$$\left(1+|\nabla'\eta'|^2\right)^{\frac{1}{2}}\frac{\partial}{\partial n'}\frac{1}{r_1}=-\frac{y'+y+2h-\nabla'\eta'\cdot\mathbf{R}}{r_1^3}. \tag{60}$$

Using that $1/r_1^3=(1+\Delta^2)^{-\frac{3}{2}}/R_1^3$ (where $R_1^2=R^2+4h^2$ and $\Delta^2=(\eta'+\eta)(\eta'+\eta+4h)$ as above) we employ the Taylor series expansion of $(1+\Delta^2)^{-\frac{3}{2}}$. Using (46)–(47) above, we obtain for the first term in (60)

$$\begin{aligned}-\frac{(\eta'+\eta+2h)}{r_1^3}&=-\sum_{n=0}^{\infty}\frac{(-1)^n1\cdot3\cdot\cdots(2n+1)}{2^n n!\ R_1^{2n+3}}\left[(\eta'+\eta)^{n+1}(\eta'+\eta+4h)^n+2h(\eta'+\eta)^n(\eta'+\eta+4h)^n\right]\\&=\sum_{n=0}^{\infty}\frac{(-1)^{n+1}\mathcal{F}^{-1}[T(\mathbf{x}')p_n(2kh)]}{2^n n!\ (2h)^{2n+1}}\left[\sum_{m=0}^{n+1}\sum_{q=0}^{n}\binom{n+1}{m}\binom{n}{q}\eta'^{m+q}\eta^{n+1-m}(\eta+4h)^{n-q}\right.\\&\quad\left.+2h\sum_{m=0}^{n}\sum_{q=0}^{n}\binom{n}{m}\binom{n}{q}\eta'^{m+q}\eta^{n-m}(\eta+4h)^{n-q}\right].\end{aligned} \tag{61}$$

Consider now the second term in (60). Using the Taylor series expansion of $(1+\Delta^2)^{-\frac{3}{2}}$ ($\Delta^2<1$), we obtain

$$\frac{\mathbf{R}}{r_1^3}=\mathbf{R}\sum_{n=0}^{\infty}\frac{(-1)^n1\cdot3\cdot\cdots(2n+1)(\eta'+\eta)^n(\eta'+\eta+4h)^n}{2^n n!\ R_1^{2n+3}}, \tag{62}$$

while the gradient of (46) becomes (with n replaced by $n+1$)

$$\frac{\mathbf{R}}{R_1^{2n+3}}=-\frac{1}{2n+1}\nabla'\frac{1}{R_1^{2n+1}}=\frac{\mathcal{F}^{-1}[\mathrm{i}\mathbf{k}T(\mathbf{x}')p_{n-1}(2kh)]}{1\cdot3\cdot\cdots(2n+1)(2h)^{2n-1}}, \tag{63}$$

giving

$$\nabla'\eta'\cdot\frac{\mathbf{R}}{r_1^3}=\sum_{n=0}^{\infty}\sum_{m=0}^{n}\sum_{q=0}^{n}\frac{(-1)^n\binom{n}{m}\binom{n}{q}\eta^{n-m}(\eta+4h)^{n-q}\eta'^{m+q}\nabla'\eta'\cdot\mathcal{F}^{-1}[\mathrm{i}\mathbf{k}T(\mathbf{x}')p_{n-1}(2kh)]}{2^n n!(2h)^{2n-1}} \tag{64}$$

By carrying out the integration over the $\mathbf{x}'$-variable we obtain, similarly as in (57),

$$\frac{1}{2\pi}\int\limits_{\mathbf{x}'}\widetilde{\phi}'\frac{\partial}{\partial n'}\frac{1}{r_1}\mathrm{d}S=\Psi^{(1)}(\widetilde{\phi})+\sum_{n=0}^{\infty}\Psi^{(n+2)}(\widetilde{\phi},\eta), \tag{65}$$

where $\Psi^{(1)}(\widetilde{\phi},\eta) = -\mathcal{F}^{-1}[\mathrm{e}^{-2kh}\mathcal{F}(\widetilde{\phi})]$, and, for $n \geq 0$,

$$\begin{aligned}\Psi^{(n+2)}(\widetilde{\phi},\eta) = &\sum_{m=0}^{n+1}\sum_{q=0}^{n}\binom{n+1}{m}\binom{n}{q}\eta^{n+1-m}(\eta+4h)^{n-q}\frac{(-1)^{n+1}\mathcal{F}^{-1}[\mathrm{e}^{-2kh}p_n(2kh)\mathcal{F}(\widetilde{\phi}\eta^{m+q})]}{2^n n!\ (2h)^{2n+1}}\\ &+2h\sum_{m=0}^{n+1}\sum_{q=0}^{n+1}\binom{n+1}{m}\binom{n+1}{q}\eta^{n+1-m}(\eta+4h)^{n+1-q}\frac{(-1)^{n}\mathcal{F}^{-1}[\mathrm{e}^{-2kh}p_{n+1}(2kh)\mathcal{F}(\widetilde{\phi}\eta^{m+q})]}{2^{n+1}(n+1)!\ (2h)^{2n+3}}\\ &+\sum_{m=0}^{n}\sum_{q=0}^{n}\binom{n}{m}\binom{n}{q}\eta^{n-m}(\eta+4h)^{n-q}\frac{(-1)^{n}\mathcal{F}^{-1}[\mathrm{e}^{-2kh}p_{n-1}(2kh)\,\mathbf{i}\mathbf{k}\cdot\mathcal{F}(\widetilde{\phi}\eta^{m+q}\nabla\eta)]}{2^n n!(2h)^{2n-1}}\end{aligned} \tag{66}$$

References

1. Haver S (2004) A possible freak wave event measured at the Draupner jacket. In: Rogue Waves 2004, pp 1–8. http://www.ifremer.fr/web-com/stw2004/rw/fullpapers/walk_on_haver.pdf. Accessed 1 Jan 1995
2. Karunakaran D, Bærheim M, Leira BJ (1997) Measured and simulated dynamic response of a jacket platform. In: Guedes-Soares C, Arai M, Næss A, Shetty N (eds) Proceedings of 16th international conference on offshore mechanics and arctic engineering, vol II. ASME, New York, pp 157–164
3. Trulsen K (2006) Weakly nonlinear and stochastic properties of ocean wave fields. Application to an extreme wave event. In: Grue J, Trulsen K (eds) Waves in geophysical fluids. CISM Courses and Lectures No 489. Springer, New York, pp 49–106
4. Melville WK, Romero L, Kleiss JM (2005) Extreme wave events in the Gulf of Tehuantepec. Proceeding of Hawaiian Winter Workshop. University of Hawaii at Manoa, January 24–28
5. Grue J, Romero L, Kleiss JM, Melville WK (2008) Orbital velocity in spatial ocean wave elevation measurement: nonlinear computation and approximation. In: International conference on offshore mechanics and arctic engineering. OMAE2008, June 15–20, Estoril, Portugal
6. Zakharov VE (1968) Stability of periodic wave of finite amplitude on the surface of a deep fluid. J Appl Mech Phys Engl Trans 9:190–194
7. Clamond D, Grue J (2001) A fast method for fully nonlinear water wave computations. J Fluid Mech 447:337–355
8. Grue J (2002) On four highly nonlinear phenomena in wave theory and marine hydrodynamics. Appl Ocean Res 24:261–274
9. Fructus D, Clamond D, Grue J, Kristiansen Ø (2005) An efficient model for three-dimensional surface wave simulations. Part I: free space problems. J Comput Phys 205:665–685